System Response of Piping Configurations Under Overload Conditions

K. Kussmaul, K. Kerkhof, K.-H. Herter
MPA, Universität Stuttgart, Stuttgart, FRG

ABSTRACT

During a blowdown event the load level of feedwater piping systems is substantially determined by the closing behaviour of the feedwater valve. Under high loading the system response is considerably influenced by damping due to dissipation of energy in consequence of local plastifications.

Ruptures of feedwater piping were simulated within the scope of the HDR (Heißdampfreaktor) Safety Research Program. After blowing-up the rupture disc inelastic structural response was induced by the pressure waves according to the damping characteristic of the valve.

Comparative calculations concerning these blowdown tests are reported in this contribution. The straight piping sections were modelled with bar-elements and the pipebend areas with elbow-elements, so that the pipebending can also be considered according to the shell theory. The system response was determined with a non-linear direct time integration scheme.

Displacements and strains correspond well with the measured results. The damping influence of the local plastification on the response of the complete system is illustrated by a comparison of this elasto-plastic calculation with a purely elastic calculation as well as by means of energy diagrams (e.g. the sum of the plastic energy dissipation with respect to time).

NOMENCLATURE

a	pipe radius
d	wall thickness
I	internal force vector
M	mass matrix
P	external force vector
R	torus radius
t, Δt	time, time step
u	displacement vector
$\dot{u}$, $\ddot{u}$	derivations due to time

α, β, γ factors due to time integration

ε strain

λ geometric pipe factor

INTRODUCTION

In the framework of the Nuclear Reactor Safety Research in the Federal Republic of Germany full scale structural experiments have been performed at the decommissioned "Superheated Steam Reactor" HDR near Frankfurt /1,2/. During Phase I of the HDR-project /3/ extensive pipe testing focussed on experiments, in which the blowing up of a rupture disc simulated a large break of the main feedwater line followed by a sudden closing of a feedwater check valve /4,5/. The accompanied analyses of these experiments, especially the benchmark calculations within the project "German Standard Problem" /5/ which was directed towards one of the blowdown tests, revealed that the predictions of system responses could not satisfy in all respects. In this case, e.g. local plastifications or ovalizations of pipebends were not considered.

Because of this situation during Phase II of the HDR-project another series of blowdown tests /6/ has been carried out accompanied by advanced nonlinear finite element calculations.

This paper reports about nonlinear calculations for three blowdown experiments of HDR-project phase II /7-10/.

THE BLOWDOWN EXPERIMENTS

The piping system under investigation, Fig. 1, has fixpoints at the reactor pressure vessel and at the rupture nozzle where the rupture disc is installed. The blowdown tests discussed in this report are characterized as shown in Table 1.

Table 1: Important characteristics of the blowdown tests during HDR-project Phase II

HDR-blowdown test	T21.1	T21.3	T21.4
closing behaviour of the feedwater check valve closing time	damped 0,24 s	undamped 0,050 s	undamped 0,066 s
internal pipe pressure before blowdown	7 MPa	9 MPa	9 MPa
max. pressure peaks after blowdown (see Fig. 2 e.g.) at a point close to the SRV 350 valve	10 MPa	28 MPa	31 MPa

The objective of the first experiment T21.1 was the investigation of the system response of the feedwater line using a conventionally damped check valve. The second experiments T21.3 and T21.4 focussed on inelastic deformation, e.g. at fixpoints and pipebends, caused by increased impulse loading from undamped valve closing behaviour. The influence of damping due to local plastification on the overall system response could be identified /7/ and was verified by comparing the computational results with the measured data.

A comparison between calculation and measurement of the deformation behaviour was carried out at pipebend 1 for blowdown test T21.3 and T21.4. Numerous strain gauges were applied, e.g. 27 rectangular rosettes on the outer surface, and 2 rosettes on the inner surface of the pipe.

ANALYTICAL DEVELOPMENT OF IDEALIZATION OF PIPING SYSTEMS

The pioneering work of von Kármán /11/ was the first effort to model pipebends using beam theory and scaled stiffnesses and stresses by means of flexibility and stress-intensification factors. Beside this, ovalization of the pipe cross section could be taken into account. Whereas this approach was restricted to inplane loading of the pipebend, it was extended by Vigness /12/ to out-of-plane loading using similar procedures.

At the beginning of the use of the finite element method (FEM), fully three-dimensional elements as well as general shell elements have been used leading to high numbers of degrees of freedom in the finite element equation system. Therefore, special elbow elements have been developed in order to reduce computational expenses.

Several authors came up with a single displacement-based elbow element which models the complete pipebend as a whole. This element accounts for axial, torsional and bending displacements together with cubically varying ovalization deformations along the elbow element length.

This work finally established an elbow element which takes into account cross section warping and the transformation of ovalization into neighbouring elements /13/. Furthermore, several elbow elements can be connected in modelling one pipebend. The elements use polynomial interpolation along their length, together with Fourier interpolation around the pipe circumference to model ovalization and warping of the section.

IDEALIZATION OF THE FEEDWATER LINE

Finite element mesh

The pipe elements of the ABAQUS element library /13/ were used for the non-linear dynamic analysis of the blowdown tests.

In the straight pipe sections "PIPE31"- elements considering the membrane stresses caused by internal pressure, were used. The pipebends and the directly adjacent straight segments were modelled with "ELBOW31"-elements, featuring the above mentioned capabilities to cross section ovalization and warping as well as increasing stiffness effects caused by internal pressure.

The geometric pipe factor with $\lambda = Rd/a^2$ plays an important role for choosing the number of Fourier modes. For the piping system under consideration, this factor is in the range of $1.0 < \lambda < 1.2$. Therefore, 4 Fourier modes and 12 integration points around the circumference of an "ELBOW31"-element have been used. Through the wall thickness 5 integration points were considered. Each

pipebend was modelled by 3 "ELBOW31"-elements.

The total number of elements was mainly determined by the variations in the cross section geometry. For blowdown test T21.1 the pipe was modelled by about 50 elements and 290 nodal points. Some more elements have been used for blowdown tests T21.3 and T21.4 due to more detailed analysis of pipebend 1.

The considered masses were composed of pipe material, isolation material, and water content.

Boundary conditions

The boundary conditions at the reactor pressure vessel and at the rupture nozzle were taken as fully constraint. A verification of this assumption was performed by means of a comparision between measured and calculated natural frequencies and corresponding mode shapes /10/. Along the whole piping system there are no hangers. Kinematic boundary conditions 'No Ovalization' and 'No Warping' were set between the straight ELBOW-elements and the adjacent PIPE-elements.

Material law

The material of the feedwater line is mainly 15 NiCuMoNb 5. In some areas the materials 15 Mo 3 as well as St 35.8/III were used. The stress strain representations for the test temperature of 220°C were taken in form of a multi-linear approximation. Isotropic hardening was used to describe the material hardening behaviour.

Damping

The experimentally determined modal damping values /10/ ranged from 0,3 % to 1,0 % for the first 5 mode shapes. Therefore modal damping was neglected in the nonlinear analysis. Damping due to plastic energy dissipation was considered.

MODEL VERIFICATION BY MEASURING NATURAL FREQUENCIES AND MODES

In order to verify the analytical model (e.g. boundary conditions or local stiffness distributions), a comparison of calculated and measured natural frequencies and corresponding mode shapes is a useful tool, e.g. /14/.

For the present blowdown experiment spectral and modal analyses of elastic snap back tests were carried out. The first 5 measured and calculated natural frequencies and corresponding mode shapes were in good agreement. Table 2 shows the frequencies as well as the location and direction of the highest amplitudes according to the corresponding mode shapes.

In the system response only very low-frequency vibrations are to be expected. Therefore, the agreement between measurement and calculation of the natural frequencies and corresponding mode shapes, documented in Table 2, is sufficient.

Table 2: Natural frequencies of the piping system

mode shapes No.	measured frequency (Hz)	measured damping (%)	calculated frequency (Hz)	largest amplitude (measured and calculated) location and direction	
1	4.5	0.3	4.7	2nd pipebend	X
2	6.2	0.3	6.3	1st and 2nd pipebend	Z
3	7.5	0.4	7.9	1st pipebend	Y
4	12.7	0.7	13.8	2nd and 3rd pipebend	Y
5	16.8	1.0	18.7	3rd and 4th pipebend	Z

CALCULATION OF SYSTEM RESPONSE

Time History Dynamic Integration (THDI)

Dynamic calculations which use direct time integration schemes are monitoring static equilibrium at each time step. Solving equation (1) comprises a step integration without any prior transformation.

$$\mathbf{M}\,\ddot{\mathbf{u}} + \mathbf{I} - \mathbf{P} = \mathbf{O} \qquad (1)$$

Nonlinear dynamic problems are integrated explicitly or implicitly. Values for dynamic quantities at $t + \Delta t$ determined by explicit methods are entirely based on available values at time t. An advantage of using this method in combination with a lumped mass matrix is that no equation needs to be solved, leading to simplifications in the computer code. But, on the other hand, a reduced conditional numerical stability is a serious limitation of this approach.

Implicit methods are chosen because of their numerical stability. ABAQUS uses an implicit operator, the Hilber-Hughes operator /13/. The definition of this operator is based on the Newmark formulae for displacements and velocities:

$$\mathbf{u}(t+\Delta t) = \mathbf{u}(t) + \Delta t\dot{\mathbf{u}}(t) + \Delta t^2[(1/2-\beta)\ddot{\mathbf{u}}(t) + \beta\,\ddot{\mathbf{u}}(t + \Delta t)] \qquad (2)$$

$$\dot{\mathbf{u}}(t + \Delta t) = \dot{\mathbf{u}}(t) + \Delta t(1 - \gamma)\ddot{\mathbf{u}}(t) + \gamma\,\ddot{\mathbf{u}}(t + \Delta t) \qquad (3)$$

In ABAQUS numerical damping is controlled by a single parameter α with:

$$\beta = 1/4(1-\alpha)^2 \text{ and } \gamma = 1/2 - \alpha$$

The value of α ranges from $-1/3$ (significant numerical damping) to $\alpha = 0$ (no damping, trapezoidal rule). $\alpha = -0.05$ is a good choice for quickly removing high-frequency noise without having significant effects on the low-frequency response /13/. The Hilber-Hughes operator replaces the actual equilibrium equation (1) with a balance of d'Alembert forces at the end of the time step, and a weighed average of the static forces at the beginning and end of the time step:

$$\mathbf{M}\,\ddot{u}(t + \Delta t) + (1-\alpha)[\mathbf{I}(t + \Delta t) - \mathbf{P}(t + \Delta t)] - \alpha[\mathbf{I}(t)-\mathbf{P}(t)] = 0 \qquad (4)$$

Another important advantage of the solution technique in ABAQUS is the automatic time stepping algorithm requiring a small amount of numerical dissipation. The basis of the algorithm is to estimate discrete impact times and to solve for rapid changes in velocity and accelerations on the assumption that they occur instantaneously.

Eq. (4) is satisfied at the end of each time step Δt, thus ensuring equilibrium at these times, whereas the quality of equilibrium at intermediate time points is not specified. Therefore, 'half-step residuals' are determined for a better solution control. For calculating the 'half-step residuals', linearly varying accelerations over the time interval are assumed. With the results at $t + \Delta t$ together with Newmark's formulae, it is possible to evaluate the equilibrium residual at any time $t + \tau\Delta t$ within the step. τ is arbitrarily chosen as $\tau = 1/2$. The maximum 'half-step residual' is the magnitude of the largest entry in

$$\mathbf{R}_{1/2}(t + 1/2\Delta t) = \mathbf{M}\,\ddot{u}(t + 1/2\Delta t) + \mathbf{I}(t + 1/2\Delta t) - \mathbf{P}(t + 1/2\,\Delta t)$$

Depending on a defined tolerance value, its comparison with max. $|R_{1/2}|$ initiates a time step increase respectively decrease if this value is exceeded.

Loading

As earlier investigations already have shown /3/, the use of pressure vs. time values as load input for a blowdown analysis gives good results, and fluid-structure interactions can be neglected.

For the present calculations, the task was to use measured pressure-time functions at 8 different locations in the piping system as load input. Therefore, to each element of the FE-mesh the data of the closest measurement point were assigned. The load-important fluid-dynamic process is limited to a very short time duration. Afterwards, from approximately 300 ms ($\pm$ 150 ms) after blowdown depending on the internal pressure vs. time function oscillating effects of the fluid column are dominating. A constant pressure according to the level of the water column was taken for load-input.

VERIFICATION OF CALCULATIONAL RESULTS BY COMPARISON OF MEASUREMENT AND CALCULATION

In the system response essentially only the first two mode shapes were excited. Plastification occurred close to the fixpoints and in the flank of pipebend 1 during blowdown tests T21.3 and T21.4. The vibrating and deformation behaviour was monitored by 145 high temperature strain gauges (76 in pipebend 1) applied and several displacement- and acceleration-measurements. Detailed comparisons between measurement and calculation due to all blowdown-tests are given in /7-10/ showing in most cases a good agreement. The vertical displacements of pipebend 1 and the longitudional strain history at a point close to the fixpoint at the reactor pressure vessel are shown in Figs. 3 and 4.

The measured and calculated hoop strain history at the inside and outside surface in the flank of pipebend 1 are compared in Fig. 5. The material 15 NiCuMoNb 5 yields at ε=2.5 ‰. Inelastic strains due to ovalization occurred. The automatic time stepping of ABAQUS is also documented in Fig. 5. The time step size Δt varies between 10 ms and 0.17 ms. The latter occurred between the 9th and 10th time step at the first peak point of displacements.

In Fig. 6 the strain distributions at the outside wall surface at the time step

of maximum loading after blowdown are shown for the cross-section Q_6 (see Fig. 1) as a function of the hoop angle. Measured and computed values in axial and hoop direction are compared. The greater differences between measurement and calculation during blowdown test T21.4 compared with blowdown test T23.3 are established in remaining plastic strains and corresponding material hardening during the previous blowdown test T21.3. This effect could not be taken into account as initial condition.

ENERGY DISSIPATION DUE TO PLASTIFICATION

By means of the calculations verified in the steps mentioned above energy dissipations can be determined quantitatively. The energy dissipations amounted approximately to 0.01 MNm in test T21.1 and approximately to 0.03 MNm in test T21.3 and 0.18 MNm in test T21.4, as shown in Figs. 7 and 8. The energy dissipations were much higher in test T21.3 compared with test T21.1. Despite of much larger loads (see Fig. 2), the maximum displacements, e.g. the vertical ones of pipebend 1 with 67 mm were situated only slightly above those of test T21.1 with 57 mm.

The behaviour of the feed water line without system damping, e.g. by means of test T21.1 is shown in Fig. 9. The vertical displacements of the first pipebend of the elastic-plastic calculation are compared with those of a linear calculation. It becomes evident, that a resonance effect would occur, if a material of higher strength would be chosen at the fix points.

CONCLUSION

The system response of a piping system with a system pressure of 7 resp. 9 MPa led to internal pressure shock waves up to 10 resp. 31 MPa. The formation of yielding hinges with stiffness decrease and equivalent corresponding high amplitudes of vibration did not occur. However, the displacements remained limited due to energy dissipation.

The comparison of elastic-plastic calculations was in satisfactory agreement with the measurements and allowed a further, especially energetic interpretation of structure responses. Herewith safety reserves can be quantified. Additionally investigations especially to system responses with longer durations are still needed.

ACKNOWLEDGEMENTS

The authors wish to express their appreciation to the management of the HDR-Safety-Program as well as to Bundesministerium für Forschung und Technologie (BMFT), Bonn, for sponsoring the investigations.

REFERENCES

/1/ Kussmaul, K.:
"Beanspruchungs- und Versagensuntersuchungen an Druckbehältern und Rohrleitungen",
7. Statusbericht des Projektes HDR-Sicherheitsprogramm des Kernforschungszentrums Karlsruhe, Dezember 1983

/2/ Kussmaul, K.:
"Stress and Failure Studies Related to the HDR Pressure Vessel and Piping",
Nuclear Engineering and Design 88, No. 3, pp. 261/76, 1985

/3/ HDR-Sicherheitsprogramm, Gesamtprogramm Phase I, Rev. 4,
Kernforschungszentrum Karlsruhe, Jan. 1982

/4/ Meier, D., Hunger, H.:
"Untersuchungen über die Reaktion und Beanspruchung einer Rohrleitung mit Speisewasserrückschlagventil bei Kühlmittelverluststörfällen",
Auswertebericht Versuchsgruppe SRV 350, PHDR Technischer Fachbericht Nr. 43-84, November 1984

/5/ Deutsches Standard-Problem Nr. 4a,
"Dynamisches Strukturverhalten einer Rohrleitung mit Rückschlagventil bei Blowdown",
HDR-SRV 350 Versuch Nr. 60.4.1 Strukturdynamik, Dezember 1984

/6/ Hunger, H.:
Auslegungsbericht "Rohr-Blowdownversuche mit Ventilschließen",
HDR-Versuchsgruppe RORB T21.0, T21.1, T21.3,
PHDR-Arbeitsbericht Nr. 2.174/85, September 1985

/7/ Diem, H., Hunger, H.:
"Überelastische Rohrverformung unter scharfer Drucklast bei Blowdown mit ungedämpftem Ventilschließen",
10. Statusbericht, HDR Sicherheitsprogramm, Dezember 1986

/8/ Kerkhof, K., Diem. H.:
Detailnachrechnung und Auswertung des Blowdownversuchs T21.3,
MPA-Bericht 815 512 Ke/Dm, November 1988

/9/ Kerkhof, K.:
Nachrechnung des Blowdown-Versuchs T21.4 mit dem Programm ABAQUS,
MPA-Bericht 815 516 Ke/Ef, November 1987

/10/ Firnhaber, M., Müller, W.Ch.:
"Dynamisches Strukturverhalten einer Rohrleitung mit Rückschlagventil bei Blowdown", Vergleichsrechnung (DSP) Nr. 9, GRS-A-1486, Gesellschaft für Reaktorsicherheit, Köln, September 1988

/11/ v. Kármán, T.:
"Über die Formänderung dünnwandiger Rohre, insbesondere federnder Ausgleichsrohre",
Zeitschrift des Vereins Deutscher Ingenieure, Vol. 55, 1911, pp. 1989-1995

/12/ Vigness, I.:
"Elastic Properties of Thin-Walled Curved Tubes of Short-Bend Radius",
TRANS. ASME, VOL. 73, 1951, PP. 74-84

/13/ ABAQUS USER Manual and Theory Manuals, Versions 4.5 and 4.6
Hibbit, Karlsson & Sorenson Inc.

/14/ Luz, E., Kerkhof, K.:
"Natural Frequencies and Mode Shapes of the Bridge over the Kocher-Valley",
Final Report 12th IABSE Congress, Vancouver, Sept. 1984

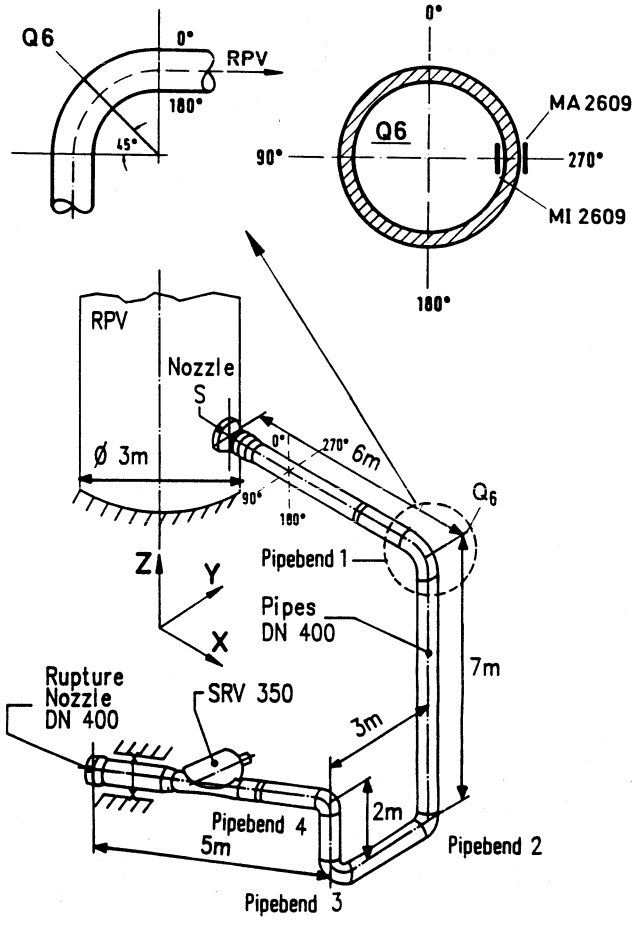

Fig. 1: Isometry of the investigated piping system

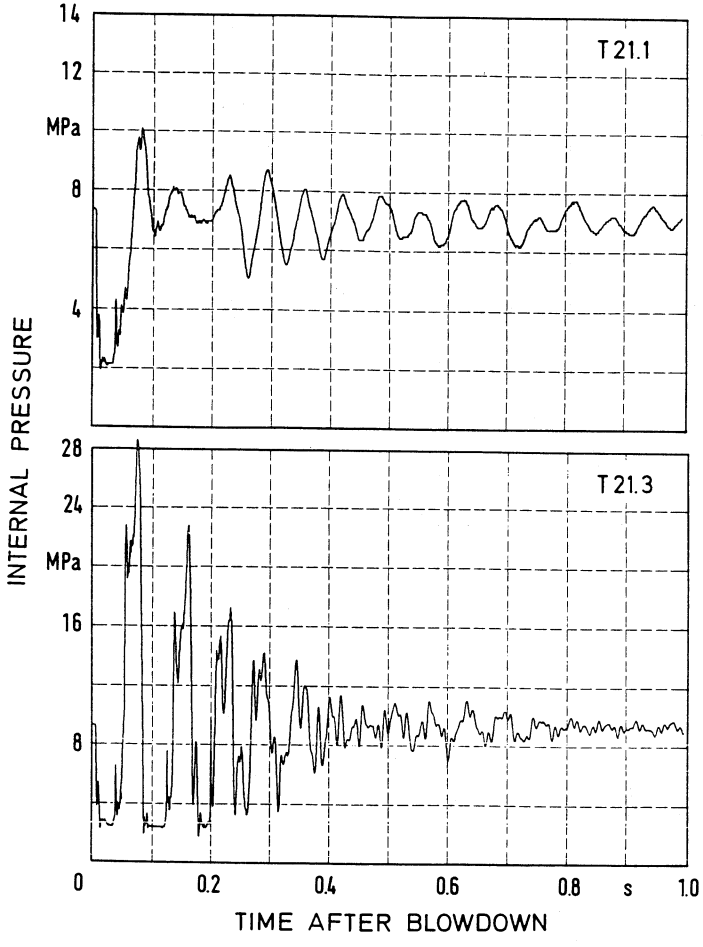

Fig. 2: Internal pressure, measured at a point close to the valve SRV 350

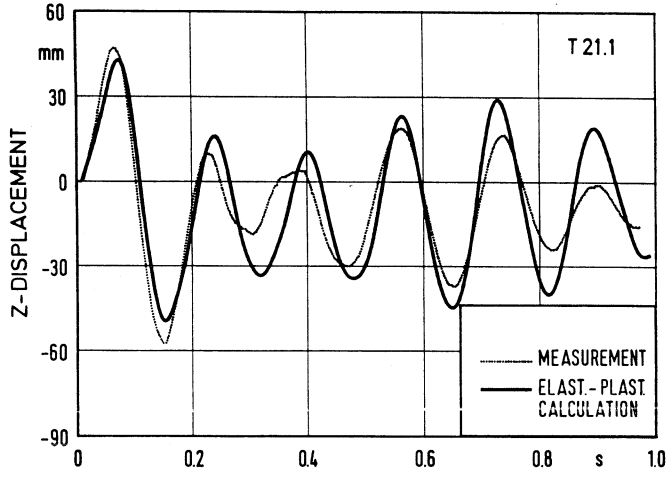

Fig. 3: Vertical displacements of pipebend 1

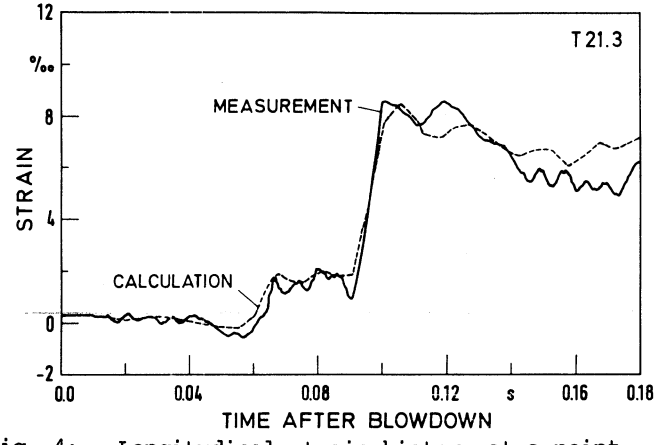

Fig. 4: Longitudinal strain history at a point close to the RPV

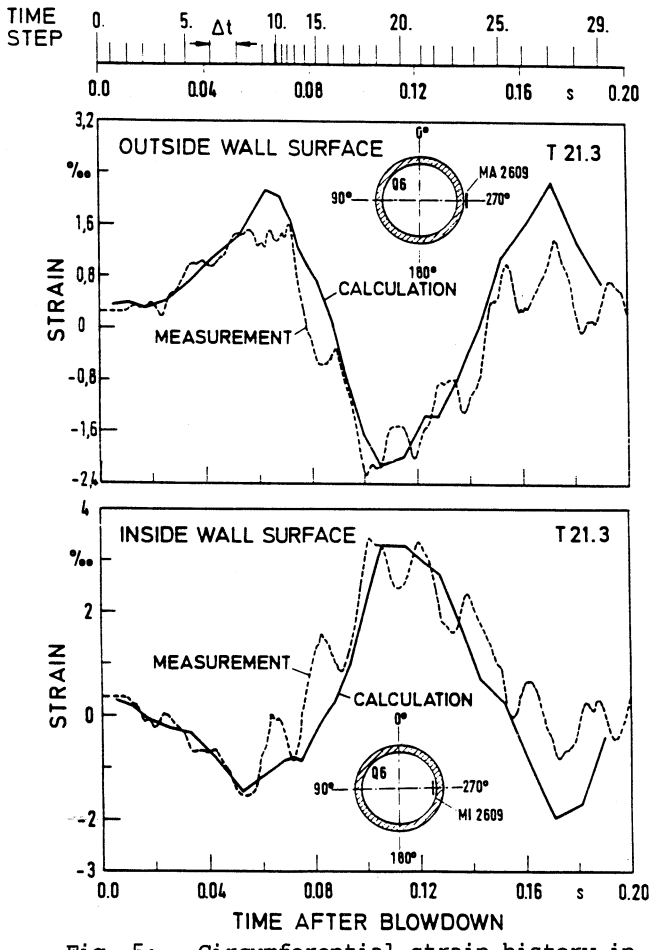

Fig. 5: Circumferential strain history in the flank of cross-section Q6

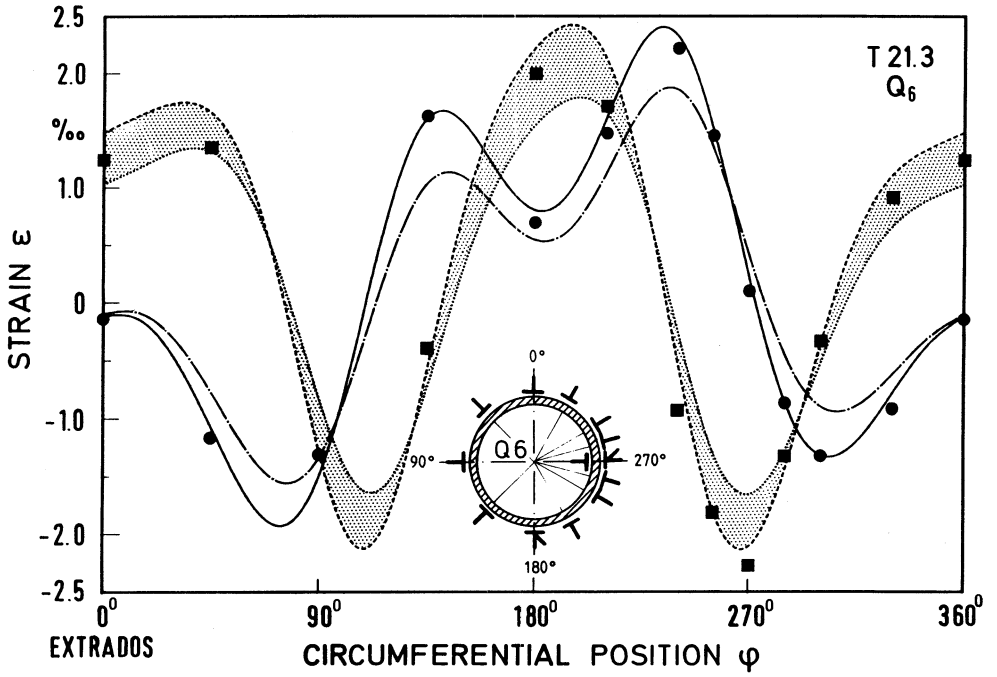

	CALCULATION	MEASURE-MENT
CIRCUMFERENTIAL STRAIN	19. TIME STEP 18. TIME STEP	■

	CALCULATION	MEASURE-MENT
LONGITUDINAL STRAIN	19. TIME STEP 18. TIME STEP	●

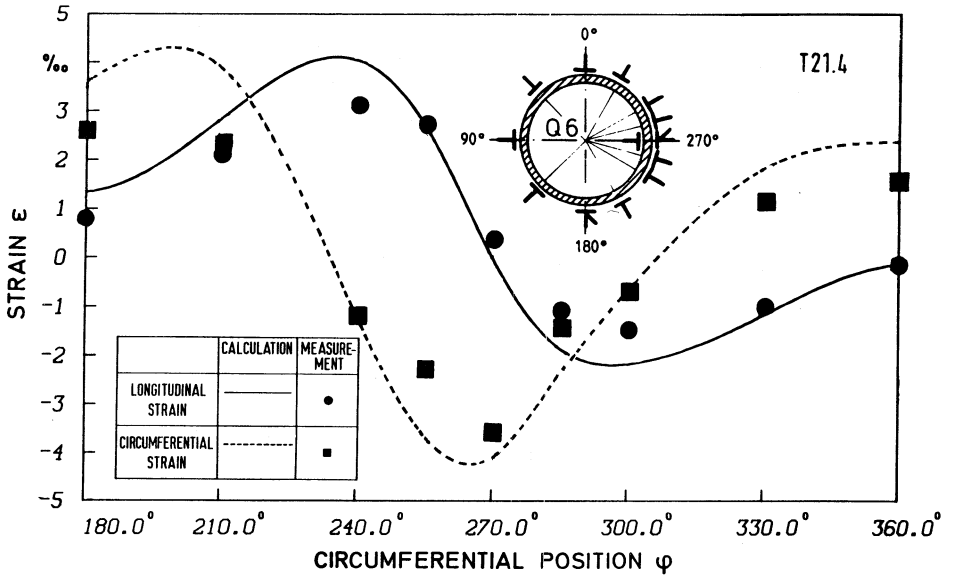

Fig. 6: Surface strains in cross-section Q6 at 0.10 s (T21.3) resp. 0.13 s (T21.4) after blowdown

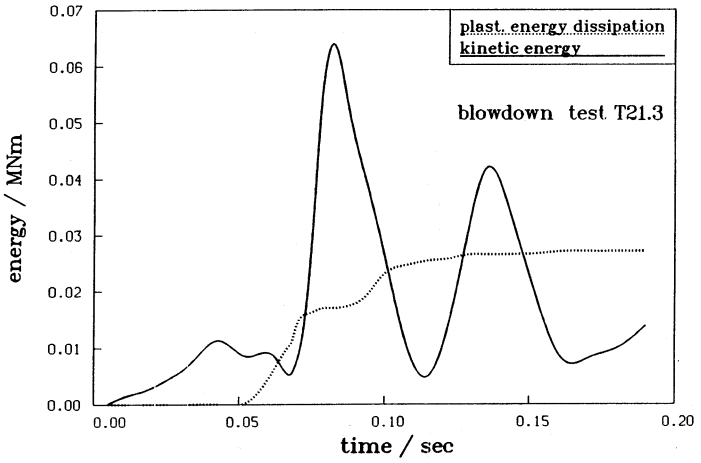

Fig. 7:

Energy diagram

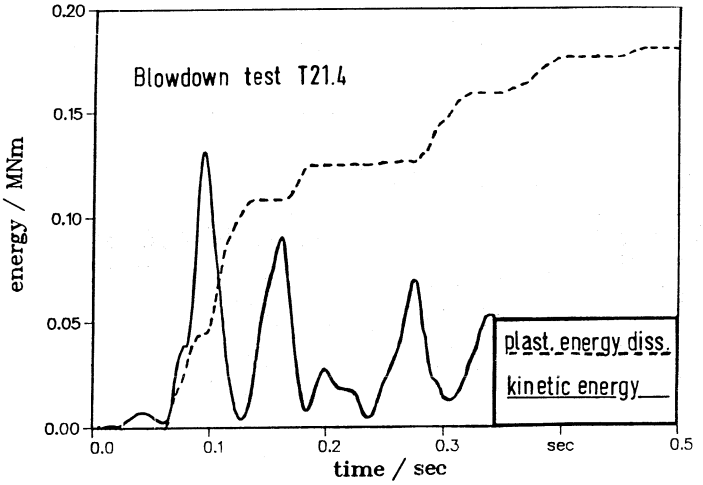

Fig. 8:

Energy diagram

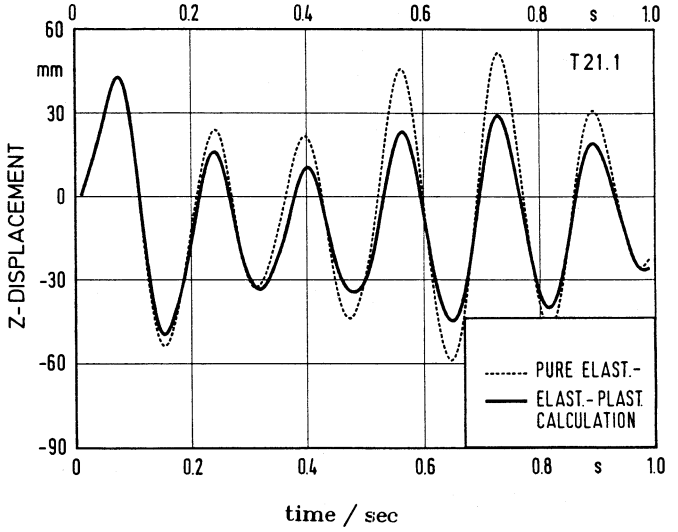

Fig. 9:

Vertical displacements of pipebend 1

comparison of elastic with elastic-plastic calculation